



The Physical Thickness of Stellar Disks to

$$Z \sim 2$$

arXiv:2303.04171v1

Reporter: Jiayu QI (戚嘉妤)

2024-04-19

OUTLINE

- Introduction
- Data and Sample Selection
- Measurements
- Results
- Conclusion

Introduction

- **Older stars** are generally found **at larger distances** above and below the galaxy midplane than their younger counterparts (Wyse & Gilmore 1995; Holmberg et al. 2009; Leaman et al. 2017).
- **The older stars** in the Milky Way **comprise “thick disk”** (with a scale height of ~ 1 kpc), while **its gas and younger stars comprise** its flatter **“thin disk”** (scale height ~ 270 pc) (Gilmore & Reid 1983; Bland-Hawthorn & Gerhard 2016).
- **Most disk galaxies** in the local universe appear to **have a thick(-er) disk** component made up of **old(-er) stars** (Yoachim & Dalcanton 2006).

Introduction

- **The classic explanation** for thick disks assumed that the stars first form in thin disks that gradually thicken with time through dynamical heating.
- **The recent explanation** contends that stars form in thick disks at early times and in progressively thinner disks at later times.
- **To distinguish** between these scenarios, one **needs direct measurements of the thicknesses** of galaxy disks back to the early universe.
- In this paper, they measure the vertical scale heights of 491 edge-on galaxies from $z \sim 0.4$ to $z \sim 2.5$ to reveal how and when galaxies formed their thick stellar disks.

2. Data and Sample Selection

2.1 HST Imaging and Catalogs

- They use **3-band optical** and **near infrared imaging** of the GOODS-S galaxy field observed with the Advanced Camera for Surveys (ACS/850LP) and the Wide Field Camera 3 (WFC3/F125W+F160W) on HST.
- They use the **image mosaics**, source detection, segmentation maps, and photometric catalogs of this imaging field as provided by the 3D-HST survey (Skelton et al. 2014).
- They adopt measurements of the F160W photometric axis ratios, position angles, and effective radii of the galaxies in GOODS-S from the **GALFIT catalogs** described in *van der Wel et al. (2012)*.

2. Data and Sample Selection

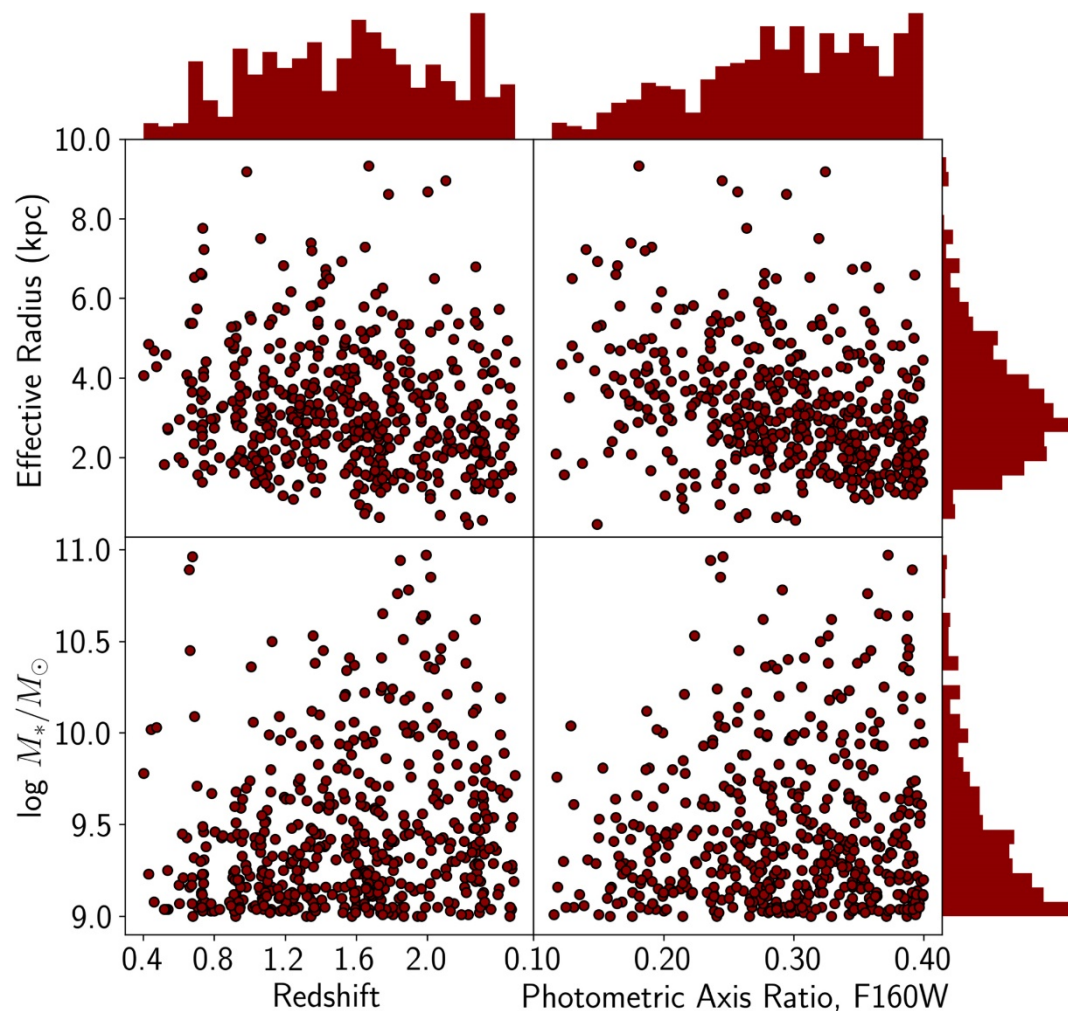


Figure 1 The distributions of stellar mass, redshift, WFC3/F160W effective radius, and WFC3/F160W photometric axis ratio.

- The **effective radius** is defined as **the semi-major axis** of the ellipse that contains half of the total light in the best fitting GALFIT single-Sérsic model.
 - The **axis ratio** is defined as **the ratio of the semi-major and semi-minor axes** from the best-fitting Sérsic model (van der Wel et al. 2012).
- The majority of the galaxy sample have low stellar mass ($9 < \log M^*/M_\odot < 10$).

2. Data and Sample Selection

2.2 Galaxy Sample Selection

- First, they select a parent sample of **6933 galaxies** that span a fixed range in mass ($\log M^*/M_\odot = 9-11$) and photometric redshift ($Z_{\text{phot}} = 0.4 - 2.5$).
- From the parent sample, **they use two criteria** to select galaxies with a well-defined orientation, i.e., a well-defined major and minor axis, so that they can orient the plane of the galaxy.
- They compare the position angle measured by the 3D-HST team using the SExtractor code (Bertin & Arnouts 1996) to that measured from GALFIT for each galaxy.
- They remove 3 galaxies with errant effective radii (> 5 arcsec).

Together, these criteria reduce the sample to **3032 galaxies**.

2. Data and Sample Selection

2.2 Galaxy Sample Selection

- To mitigate projection effects in the scale height measurements, they want to use galaxies whose disks are oriented perfectly **edge-on** relative to our line of sight (LOS).
- They consider a galaxy sufficiently edge-on if it has an F160W photometric axis ratio of **$b/a \leq 0.4$** .
- They then use simulations of randomly-inclined galaxy disks to calculate the bias to the median of the measured scale heights due to the residual inclination.
- Finally, they remove galaxies with a close neighbor ($< 2''$) in the full 3D-HST source catalog.
- An additional 36 galaxies were discarded due to bad surface brightness fits.

The final sample includes 491 galaxies.

3. Measurements of Galaxy Scale Height

- For each galaxy in the sample, they extract $4 \times 4''$ postage stamps.
- In each stamp, they use the segmentation map to mask extraneous sources and identify background pixels.
- They rectify the postage stamps so that the major axis of the galaxy (i.e., the disk midplane, as defined by the F160W photometric position angle) lies along the horizontal direction of the image.

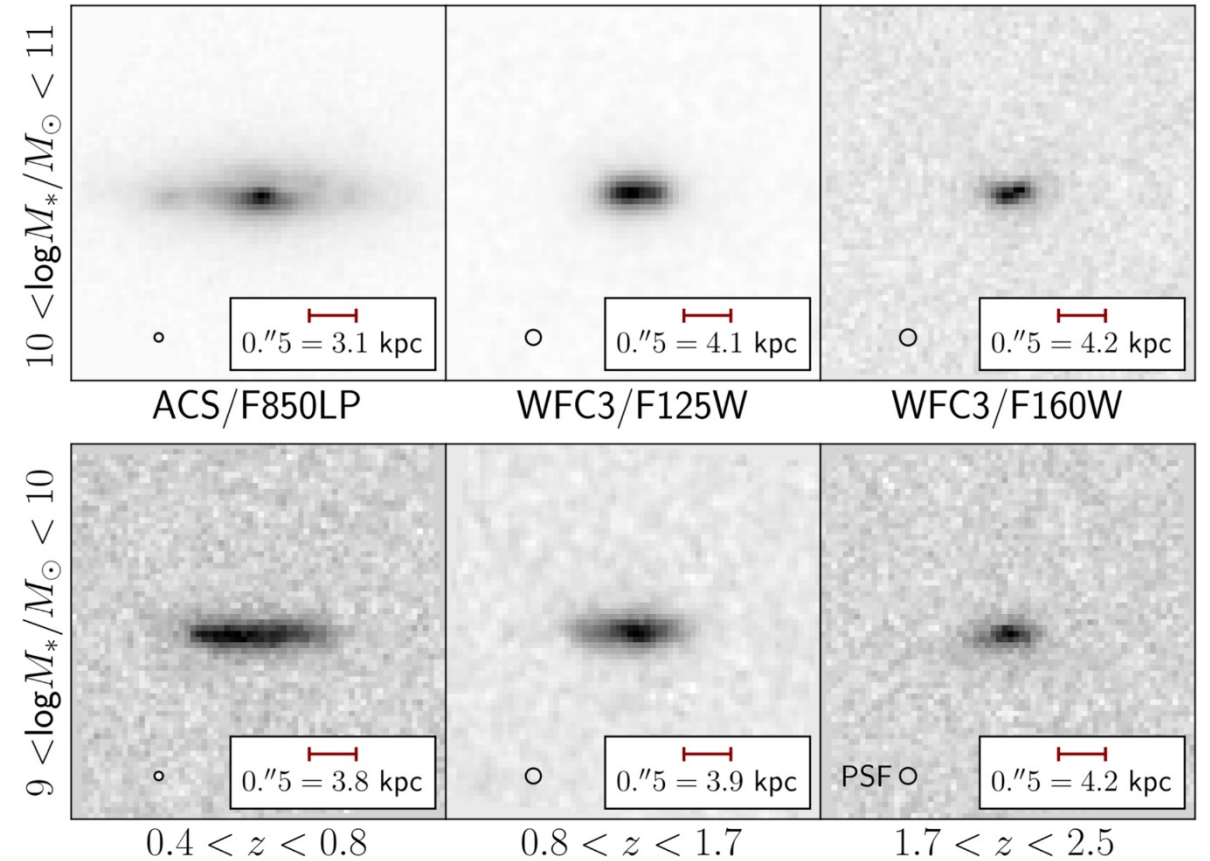


Figure 2. The HST imaging for a random subset of galaxies in the sample.

3. Measurements of Galaxy Scale Height

- They extract vertical surface brightness (and uncertainty) profiles along each column of the postage stamps. The columns are separated by $0.''06$ —which corresponds to 0.33 kpc at $z = 0.4$ and 0.52 kpc at $z = 2$.
- They fit each of the observed surface brightness profiles using a model that includes a 1D convolution of the HST point-spread function (PSF) and a 1D sech^2 surface brightness profile,

$$\text{sech}^2(A, z, z_0) = A \times \frac{4}{(e^{\Delta z/z_0} + e^{-\Delta z/z_0})^2} \quad (1)$$

- The sech^2 profile assumes that the **stars are distributed above and below the disk isothermally** (van der Kruit & Freeman 2011).

3. Measurements of Galaxy Scale Height

- For galaxies in sample that are intrinsically prolate, the “**scale height**” that they measure represents **the physical thickness of the short axis** of the system.
- For each galaxy in their sample, they measure the scale height using the imaging band that covers a **fixed rest wavelength window (0.46 – 0.66 μm)** at the redshift of the source (Figure 3).
- For each galaxy, they carry out measurements in the filter appropriate for its redshift: F160W for $1.7 < z \leq 2.5$, F125W for $0.8 < z \leq 1.7$, and F850LP for $0.4 \leq z \leq 0.8$.

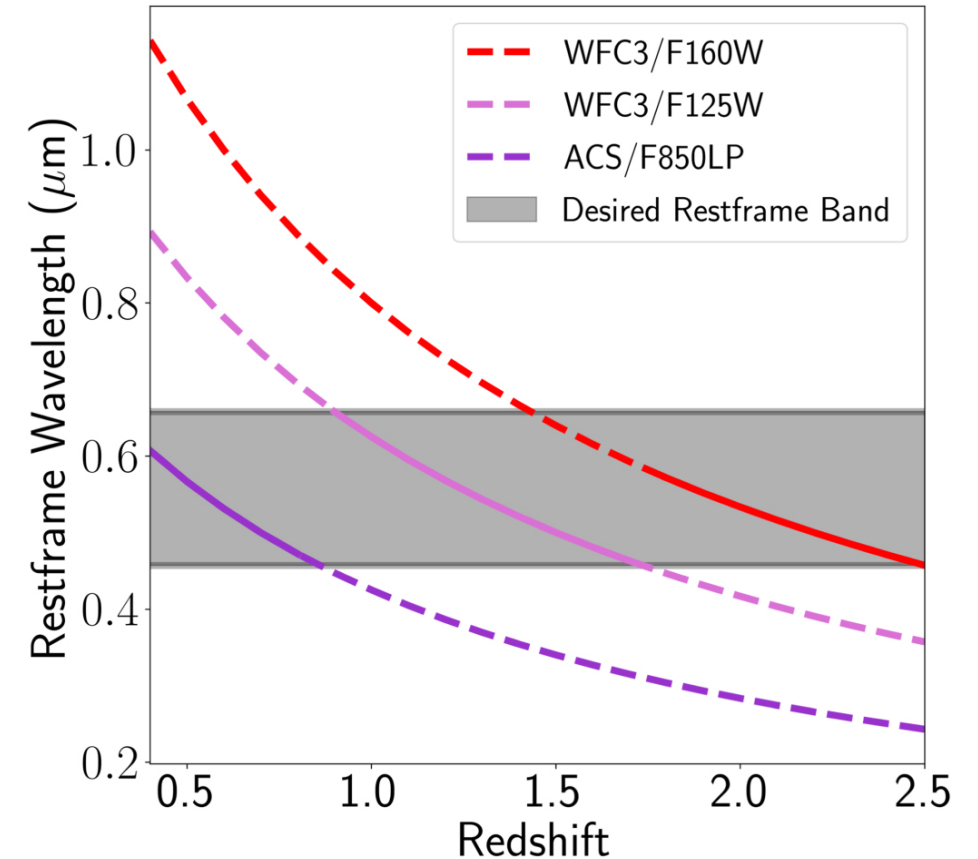


Figure 3. the redshift evolution of the rest wavelength.

3. Measurements of Galaxy Scale Height

- For each column of each galaxy, they employ the Bayesian *Markov chain Monte Carlo* (MCMC) Python package *emcee* (Foreman-Mackey et al. 2013) to derive the **probability distribution of the scale height**.
- For consistency among galaxies, **they measure the scale height as the values at the effective radius**. The effective radius is marked by the brown vertical line.
- **A circle indicating the full-width at half-maximum** of the 2D point-spread function (PSF) of the HST /WFC3 image in Figure 4.
- They note that the observed surface brightness profile is broadened beyond the 1D PSF. **This indicates a physical thickness that is detectable with the HST image.**

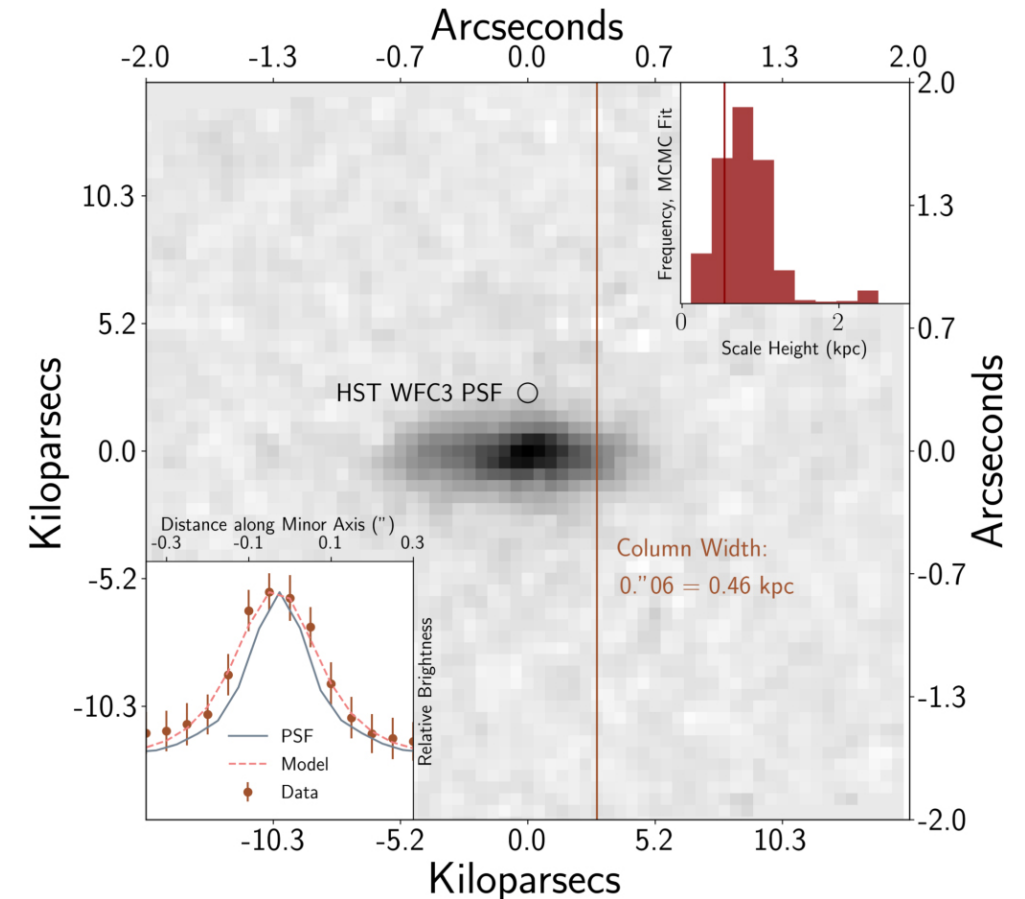


Figure 4 The results of the fit for a single column of an example galaxy ($\log M^*/M_\odot = 9.5$ at $z = 0.90$).

4. Results

- The left panel shows the scale heights and uncertainties of the full sample as a function of redshift (lookback time).
- **The red-shaded region** shows the median and the 16th – 84th percentile span of the sample running with lookback time.
- **The solid red line** shows the measured median of the population, and the **dashed red line** shows the median corrected for the average inclination of the galaxy sample.

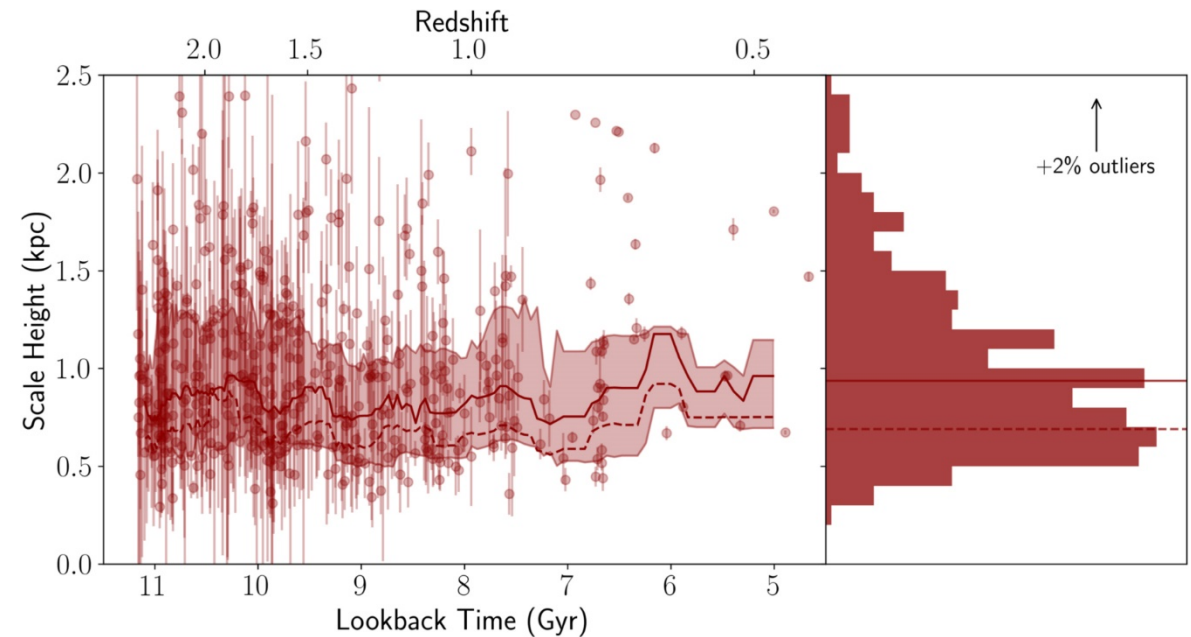


Figure 5 The scale heights of the galaxy sample.

- The right panel shows the distribution of sample with **the median** and **inclination-corrected median** marked—0.94 (± 0.04 ; standard error on the median) kpc and 0.74 (± 0.03) kpc.
- They do not find evidence for an evolution in either the median or the scatter of the population with redshift—**the red shaded region in the left panel is flat.**
- **The median galaxy scale height** of the sample is **generally constant** over a large period of cosmic time ($0.4 \leq z \leq 2.5$).

4. Results

- For the full sample, They measure a span of 0.6 to 1.4 kpc (16th – 84th percentiles) or a 1σ scatter of 0.35 kpc.
- **They split the sample into three redshift bins.** At high ($1.7 < z \leq 2.5$) and intermediate ($0.8 < z \leq 1.7$) redshifts, the median scale heights of the sample are 0.96 ± 0.07 kpc and 0.88 ± 0.04 kpc, respectively. At low redshift ($0.4 \leq z \leq 0.8$) the median scale height is 1.15 ± 0.15 kpc.
- The inclination-corrected median scale heights of the three bins are $0.75 (\pm 0.05)$, $0.69 (\pm 0.03)$, and $0.90 (\pm 0.12)$ kpc, respectively. See **Table 1** for a summary.

In Table 1, the scatter (Δz_0) is defined as $(z_{0,84th} - z_{0,16th})/2$.
The reported uncertainties are the standard error on the median.

Table 1			
z	$z_{0,\text{median}}$	$z_{0,\text{median}}^{\text{incl-corr}}$	Δz_0
(kpc)			
$1.7 < z \leq 2.5$ (N = 198)	0.96 ± 0.07	0.75 ± 0.05	0.47
$0.8 < z \leq 1.7$ (245)	0.88 ± 0.04	0.69 ± 0.03	0.40
$0.4 \leq z \leq 0.8$ (48)	1.15 ± 0.15	0.90 ± 0.12	0.80
$0.4 \leq z \leq 2.5$ (491)	0.94 ± 0.04	0.74 ± 0.03	0.35

4. Results

- The high-redshift distribution of their sample is shown in red, and the low-redshift distribution from SDSS is shown in blue.
- The median and inclination-corrected median of their high redshift sample are shown with solid and dashed red lines. The median of the local sample is indicated with a vertical blue line.
- They show the range of estimates of the scale heights of the thin and thick disks of the Milky Way (Bland-Hawthorn & Gerhard 2016).

To conclude:

Figure 6 shows that the **inclination-corrected median** of the high redshift population (0.74 ± 0.03 kpc) **is consistent with** the range of estimates (0.63–1.08 kpc) of **the Milky Way thick disk** but is **smaller than** that of **the disk galaxies** today (~ 1500 pc).

The **thin disk of the Milky Way** is significantly **thinner than** both the **high redshift** and the **SDSS** comparison samples.

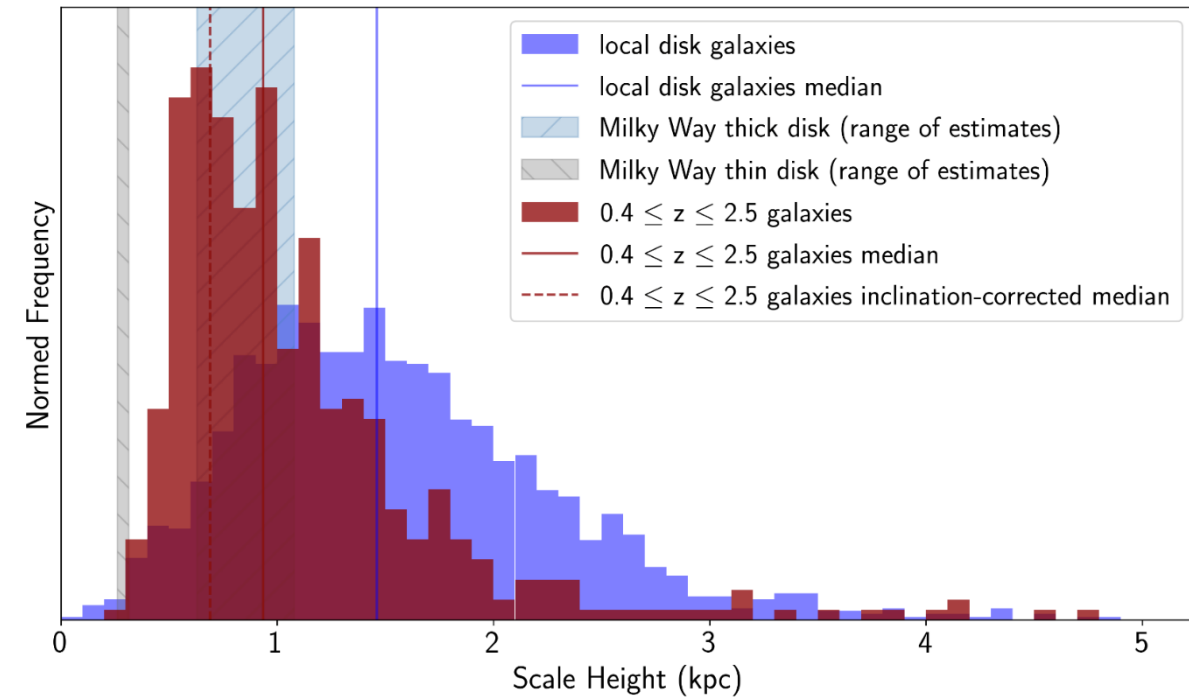


Figure 6 Comparing the distribution of the scale heights of their high-redshift galaxy sample with those of a population-matched sample of disk galaxies in the local universe as measured from the SDSS (Bizyaev et al. 2014).

4. Results

Next they consider differences in the shapes of the distributions.

- The low-redshift distribution includes an offset in the median, which is also wider than that of the high-redshift distribution. The (16, 50, 84)th percentiles of the SDSS and high-redshift distributions are (0.87, 1.46, 2.25) kpc and (0.60, 0.94, 1.52) kpc, respectively.
 - They compute **the width of the two distributions** ($p_{84} - p_{16}$) as 1.39 and 0.91 respectively.
1. The differences in the median and width of the distributions imply that with cosmic time **the disk population** needs to both (i) on average **become physically thicker** and also (ii) develop higher variety with **some galaxies remaining thin** and **some thickening**.
- They also note that both distributions contain a tail towards higher scale heights, and that the tail extends further in the low redshift distribution.
2. This implies that the **thickness of the thickest galaxies** at a given redshift **increases with decreasing redshift**.

4. Results

Draw two conclusions:

1. Disks as thick as the Milky Way are established as early as cosmic noon at $z \sim 2$.
2. These high-redshift stellar disks are as thin or thinner than their (expected) descendant galaxies today.

This indicates the thickest components of today' s galaxy disks start thick and subsequently thicken at later times.

5. Conclusion

- They use the **direct measurements of the thicknesses** of galaxy disks back to the early universe to distinguish two competing models.
- They use a large sample of galaxies ($N = 491$) and focus on a **fixed rest-optical wavelengths** to mitigate degeneracies between scale height, stellar age, and redshift.
- They compare with a population-matched sample of disk galaxies at $z = 0$ to infer evolution.
- From $z \sim 2.5$ to $z \sim 0.4$, they find **no evidence for an evolution** in the median and scatter of the scale heights of the galaxy population with redshift and **they lack the sample at $Z < 1$** .
- Their results indicate **that the stellar disks of galaxies both start thick and subsequently thicken with time**.